A Novel Bisretinoid of Retina Is an Adduct on Glycerophosphoethanolamine

Kazunori Yamamoto,[1] *Kee Dong Yoon,*[1] *Keiko Ueda,*[1] *Masaru Hashimoto,*[2] *and Janet R. Sparrow*[1,3]

Purpose. Fluorescent bisretinoid compounds accumulate in retinal pigment epithelial (RPE) cells as a consequence of two processes: random reactions of vitamin A aldehyde in photoreceptor cell outer segments, and phagocytosis of discarded photoreceptor outer segment discs by RPE. The formation of bisretinoid is accentuated in some forms of retinal degeneration. The detection of a novel bisretinoid fluorophore that is a conjugate of all-*trans*-retinal and glycerophosphoethanolamine is reported.

Methods. Human RPE/choroid, eyes harvested from *Abca4* (ATP-binding cassette transporter 4) null mutant mice, and biosynthetic reaction mixtures were analyzed by ultra performance liquid chromatography coupled to mass spectrometry and by nuclear magnetic resonance spectra and spectrofluorometry.

Results. A fluorescent compound in mouse eyes and in human RPE/choroid corresponded to the product of the reaction between all-*trans*-retinal and glycerophosphoethanolamine (A2-GPE), as determined on the basis of molecular weight (*m/z* 746), absorbance (approximately 338,443 nm), and retention time. Nuclear magnetic resonance spectra were consistent with a pyridinium molecule with a glycerophosphate moiety. The emission maximum of A2-GPE was approximately 610 nm. A2-GPE accumulated with age in mouse eyes and was more abundant in *Abca4*$^{-/-}$ mice, a model of recessive Stargardt disease.

Conclusions. To date, several bisretinoids of RPE lipofuscin have been isolated and characterized, and for all of these, formation involves the membrane phospholipid phosphatidylethanolamine. Conversely, the bisretinoid A2-GPE is detected as *sn*-glycero-3-phosphoethanolamine (GPE) derivatized by two all-*trans*-retinal. The pathways by which A2-GPE may form under conditions of increased availability of all-*trans*-retinal, for instance in the *Abca4*$^{-/-}$ mouse, are discussed. (*Invest Ophthalmol Vis Sci.* 2011;52:9084–9090) DOI:10.1167/iovs.11-8632

The outer segment of a photoreceptor cell is composed of a stack of membranous disks in which visual pigment is housed. The lipid fraction of the disc membrane is chiefly populated by phospholipids with the major species being phosphatidylethanolamine (PE; 37.6 mol %), phosphatidylcholine (PC; 32.5 mol %), and phosphatidylserine (PS; 12.1 mol %).[1] The major fatty acids in PS and PE are stearic acid (octadecanoic acid, 18:0) and docosahexaenoic acid (DHA; 22:*6n*-3) while PC primarily features palmitic acid (16:0) and 22:*6n*-3.[2] DHA is more abundant in photoreceptor outer segment disc membrane than in any other mammalian membrane and accounts for 32%, 21%, and 32% of the fatty acid associated with PE, PC, and PS, respectively.[2] The lipid phase of the photoreceptor outer segment disc membrane is essential to the signaling functions of rhodopsin and accordingly, the phospholipid populating the surround of rhodopsin is predicted to contain a high proportion of DHA-rich phosphatidylethanolamine.[3] Indeed, studies have shown that it is the combination of a relatively small PE head-group and the bulky DHA acyl chain that allows the membrane to accommodate the conformation changes in activated rhodopsin that exposes the G protein (transducin) binding site.[4–6]

It is well known that PE in the outer segment membrane reacts with all-*trans*-retinal generated by photoisomerization of the visual chromophore 11-*cis*-retinal, to form the Schiff base adduct *N*-retinylidene-PE (NRPE).[2] The formation of NRPE likely serves to sequester all-*trans*-retinal, a reactive aldehyde. NRPE is likely also the ligand that binds the photoreceptor-specific ATP-binding cassette transporter (ABCA4/ABCR) in outer segments thereby facilitating delivery of all-*trans*-retinal to NADPH-dependent retinol dehydrogenase for reduction in the cytosol. Instead of hydrolyzing to all-*trans*-retinal and PE, NRPE can under some circumstances, react with a second molecule of all-*trans*-retinal thereby initiating a nonenzymatic synthetic pathway that leads to the formation of toxic fluorescent diretinal compounds within the lipid bilayer of the photoreceptor outer segment. These compounds include the phosphatidyl-pyridinium bisretinoid A2PE and the phosphatidyl-dihydropyridine bisretinoid, A2-DHP-PE. As a consequence of outer segment disc shedding and phagocytosis, the bisretinoid chromophores of the outer segment are deposited into the retinal pigment epithelium (RPE) where they accumulate as lipofuscin. One of these RPE bisretinoids is A2E, the fluorescent pigment that is released by phosphate hydrolysis of A2PE. Deficiency in ABCA4 leads to augmented accumulation of bisretinoid and the onset of recessive Stargardt disease, a juvenile form of macular degeneration.[7–9] Enhanced formation of bisretinoid is also caused by deficiencies in photoreceptor-specific retinol dehydrogenase[10–12] and by mutations in *ELOVL4* (elongation of very long fatty acids-4).[13]

In our chromatographic analysis of the bisretinoids of retina we detected a previously unidentified fluorescent compound in human RPE. A notable feature of this compound was the similarity of the absorbance spectrum (λ_{max}approximately 338,443 nm) to that of A2PE (λ_{max} approximately 333,448 nm) and A2E (λ_{max} approximately 333,439 nm) yet with a mass (*m/z* 746) intermediate between A2E and A2PE. We report here the characterization of this compound.

From the Departments of [1]Ophthalmology, and [3]Pathology and Cell Biology, Columbia University, New York, New York; and [2]Faculty of Agriculture and Life Science, Hirosaki University, Hirosaki, Japan.

Supported by National Institutes of Health Grants EY12951 (JRS) and P30EY019007, and a grant from Research to Prevent Blindness to the Department of Ophthalmology. The Carl Marshall Reeves and Mildred Almen Reeves Foundation provided funds for equipment.

Submitted for publication September 20, 2011; revised October 19, 2011; accepted October 19, 2011.

Disclosure: **K. Yamamoto**, None; **K.D. Yoon**, None; **K. Ueda**, None; **M. Hashimoto**, None; **J.R. Sparrow**, None

Corresponding author: Janet R. Sparrow, Columbia University, Department of Ophthalmology, 630 W. 168th Street, New York, NY 10032; jrs88@columbia.edu.

METHODS

Animals and Tissues

Albino *Abca4/Abcr* null mutant mice homozygous for Rpe65 Leu450, albino *Abca4* wild type (homozygous Rpe65 Leu450), and pigmented *Abca4* wild type (homozygous Rpe65 450Met) were generated and genotyped.[14] All animals were treated in accordance with the ARVO Statement for the Use of Animals in Ophthalmic and Vision Research. Human donor eyes were received within 24 hours of death from the Eye-Bank for Sight Restoration (New York, NY). The study was in accordance with the Declaration of Helsinki with regard to the use of human tissue. Mouse eyes (four eyes per sample) and human RPE/choroid and neural retina were homogenized in DPBS using a tissue grinder in the presence of chloroform/methanol (1:1). Subsequently, the sample was extracted three times with addition of chloroform and centrifuged at 1500*g* for 5 minutes. After passage through a reversed phase cartridge (C18 Sep-Pak, Millipore, Billerica, MA) with 0.1% TFA in methanol, the extract was concentrated by evaporation of solvent under gas and was redissolved in 50% methanolic chloroform.

Ultra Performance Liquid Chromatography-Mass Spectrometry (UPLC-ESI-MS)

Mass spectrometry was performed (Waters Acquity UPLC system; Waters, Milford, MA) on a mass spectrometer that was coupled online with a single quadrupole mass spectrometer (Waters SQD) and both photodiode array (PDA; Waters) eλ and fluorescence (FLR, Waters) detectors. The mass spectrometer was equipped with electrospray ion multi-mode ionization (ESCi) and ion trap analyzer and was set to operate in either full scan mode with mass to charge ratio (*m/z*) ranging from 150 to 1400 or to scan one mass unit (selected ion monitoring). For elution, a reversed phase column (Waters XBridge C18; 2.5 μm, 3 $\times$ 50 mm) was used with a mobile phase of acetonitrile/methanol (1:1) in water with 0.1% formic acid and either A, B, or C gradient (gradient A: 70% [0–1 minute] acetonitrile/methanol; 70%–98% [1–10 minutes] acetonitrile/methanol; 98% [10–12 minutes] acetonitrile/methanol; gradient B: 70% [0–30 minutes] acetonitrile/methanol; 98% [30–55 minutes] acetonitrile/methanol; gradient C: 70% [0–1 minute] acetonitrile/methanol; 70%–98% [1–27 minutes] acetonitrile/methanol; 98% [27–50 minutes] acetonitrile/methanol; flow rate of 0.5 mL/minute. Glycerophosphoethanolamine (A2-GPE) and A2E were quantified using ultra performance liquid chromatography (UPLC) chromatograms together with software (Waters Empower 3) to determine peak areas. Molar quantity per eye was determined using calibration curves constructed from known concentrations of synthesized standards and by normalizing to the ratio of the HPLC injection volume (10 μL) versus total extract volume.

Additionally, high resolution electrospray-ionization mass spectrum was obtained with a spectrometer (Hitachi NanoFrontier LD; Hitachi, Tokyo, Japan) equipped with an HPLC pump (Hitachi 2100), a UV detector (Hitachi L-2400), a column oven (Hitachi L-2300), and an autosampler. The HPLC system was controlled by a PC equipped with a chromatography system manager (Hitachi EZChrom Elite, v 3.1). An HPLC column (Inertsil ODS-3; GL Science Japan, Torrance, CA) 2.1 $\times$ 33 mm was used.

Spectroscopy

Emission spectra of A2-GPE (30 μM) were recorded in various solvents at room temperature using a microplate reader (SpectraMax M5 Multimode; Molecular Devices, Sunnyvale, CA), quartz cuvettes (Helma; Fisher Scientific, Pittsburgh, PA). Samples of A2-GPE in water and DPBS included 0.3% dimethylsulfoxide (DMSO). Emission was recorded at 430 and 488 nm excitation. Bandpass slit was set at 3 nm. Fluorescence intensity was measured as area under the curve (Prism 4; GraphPad Software, La Jolla, CA).

NMR Spectroscopy of A2-GPE

^{1}H nuclear magnetic resonance (NMR) spectrum was obtained in CD_3OD with a JEOL spectrometer (JNM-ECA 500; Tokyo, Japan). The remaining proton signal for CHD_2OD (3.30 ppm) was used as the internal standard. Splitting patterns are described as follows: singlet (s), doublet (d), triplet (t), multiplet (m), and broad (br). ^{13}C NMR spectrum was obtained with a spectrometer (JNM-ECA 500; 125 MHz). The isotope ^{13}C in the solvent was used as internal standard (CD_3OD; 49.0 ppm).

Biomimetic Synthesis

A2E was synthesized as previously described.[15] For A2-GPE, a mixture of all-*trans*-retinal (100 mg, 351.6 μmol; Sigma-Aldrich, St. Louis, MO) and GPE (37.8 mg, 175.7 μmol; Avanti Polar Lipids, Alabaster, AL) in DMSO (3.0 mL) was stirred in the presence of acetic acid (0.8 mL, 14.1 mmol) at 37°C with sealed cap in the dark for 3 days. The mixture was poured into H_2O (30 mL), and the aqueous layer was extracted with ethyl acetate (30 mL, three times). The combined organic layer was washed with H_2O (30 mL twice) and brine (30 mL), dried over $MgSO_4$, and then concentrated in vacuo to give crude compound. The synthetic product was named A2-glycerophosphoethanolamine (A2-GPE), A2 referring to formation from two equivalents of vitamin A aldehyde. Pure sample (15 mg) was obtained by HPLC purification (YMC C18; 5 mm, 10 $\times$ 250 mm, Waters). The mobile phase was a gradient of acetonitrile/methanol (50:50) in water; 88%–100% (0–10 minutes) acetonitrile/methanol; 100% acetonitrile/methanol (10–40 minutes) with a flow rate of 2.3 mL/min. ^{1}H NMR: δ 1.04, 1.06 (each 6H, s,

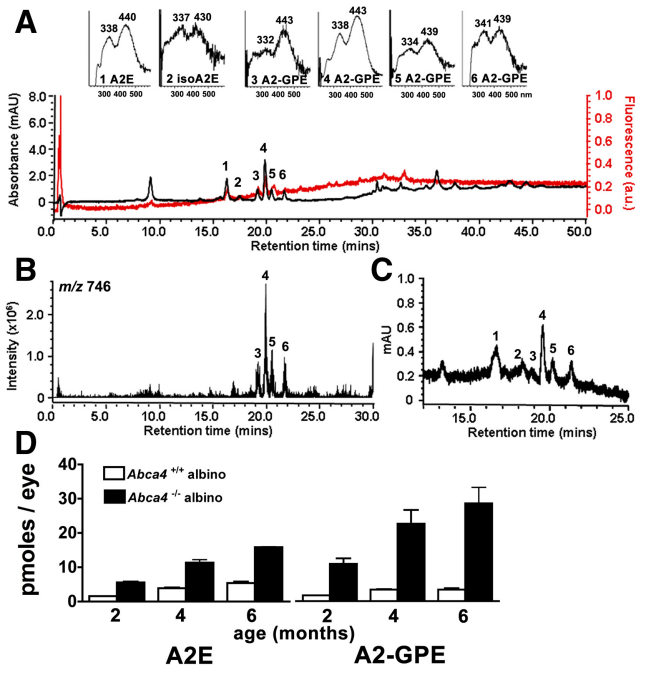

FIGURE 1. Chromatographic detection of A2-GPE. Representative reversed-phase UPLC chromatograms with 430 nm and mass monitoring. (**A**) Profile generated when injectant was a hydrophobic extract of whole *Abca4*$^{-/-}$ mice eyes, age 4 months; 4 eye cups were pooled. *Top insets*, UV-visible absorbance spectra of A2E, isoA2E, A2-GPE. (**B**) Selected ion chromatogram at *m/z* 746 with retention times corresponding to peaks 3, 4, 5, and 6 in (**A**). (**C**) Extract of RPE/choroid isolated from *Abca4*$^{+/+}$ mice; age 4 months, 14 eyes pooled. Chromatogram (430 nm absorbance monitoring) expanded between retention times 14.5–25 minutes. Peaks 1 to 6 correspond to the same numbered peaks in (**A**). (**D**) UPLC quantitation of RPE lipofuscin pigments A2E and A2-GPE in eyecups of *Abca4*$^{-/-}$ and *Abca4*$^{+/+}$ mice as a function of age. Mean $\pm$ SEM; two to three samples; 4 eye cups per sample.

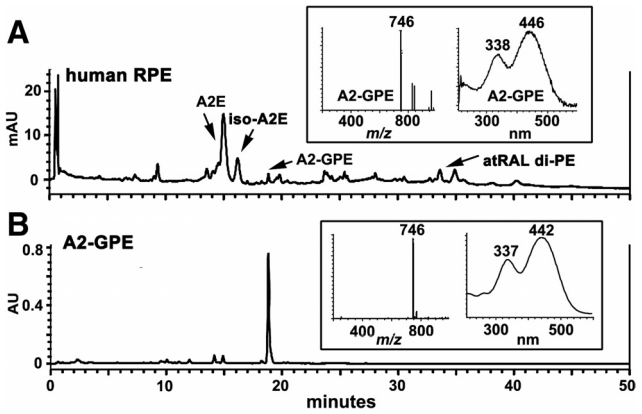

FIGURE 2. Detection of A2-GPE in human RPE. (**A**) Human RPE/choroid, donor age 54. Reversed-phase UPLC chromatogram; photodiode array detection at 430 nm; gradient C. (**B**) Synthesized A2-GPE (2 mM) exhibits the same retention time and molecular weight, and similar absorbance as A2-GPE in human RPE (**A**). *Insets*: selected ion monitoring (*m/z* 746) and UV-visible absorbance spectra.

C1-(C*H*$_3$)$_2$, C1′-(C*H*$_3$)$_2$), 1.50 (4H, m, C2*H*$_2$, C2′*H*$_2$), 1.65 (4H, m, C3*H*$_2$, C3′*H*$_2$), 1.72, 1.77 (each 3H, s, C5-C*H*$_3$, C5′-C*H*$_3$), 2.03 (3H, s, C9-C*H*$_3$), 2.05 (4H, m, C4*H*$_2$, C4′*H*$_2$), 2.15 (3H, s, C13-C*H*$_3$), 2.17 (3H, s, C9′-C*H*$_3$), 3.48, 3.53 (each 1H, dd, J = 5.4, 11.3 Hz, C*H*$_2$OH), 3.68 (1H, m, C*H*OH), 3.72, 3.78 (each 1H, m, P-O-C*H*$_2$), 4.22 (2H, dt, J = 4.7 Hz, NCH$_2$C*H*$_2$), 4.66 (2H, t, J = 4.7 Hz, NC*H*$_2$), 6.17 (1H, d, J = 16.0 Hz, C8*H*), 6.24 (1H, d, J = 11.3 Hz, C10*H*), 6.27 (1H, d, J = 16.0 Hz, C8′*H*), 6.33 (1H, d, J = 16.0 Hz, C7*H*), 6.40 (1H, d, J = 11.7 Hz, C10′*H*), 6.53 (1H, d, J = 15.9 Hz, C7′*H*), 6.64 (1H, d, J = 15.1 Hz, C12*H*), 6.71 (1H, brs, C14*H*), 6.74 (1H, d, J = 15.2 Hz, C12′*H*), 7.11 (1H, dd, J = 11.3, 15.1 Hz, C11*H*), 7.83 (1H, d, J = 2.0 Hz, C13=C*H*), 7.91 (1H, dd, J = 2.0, 6.8 Hz, C14′*H*), 7.98 (1H, dd, J = 11.7, 15.2 Hz, C11′*H*), 8.58 (1H, d, J = 6.8 Hz, C15′*H*); ^{13}C NMR (125 MHz, CD$_3$OD) δ 12.89 (C9-*C*H$_3$), 13.19 (C9′-*C*H$_3$), 15.03 (C13-*C*H$_3$), 20.24 (*C*3 or *C*3′), 20.31 (*C*3 or *C*3′), 21.93 (C5-*C*H$_3$ or C5′-*C*H$_3$), 21.96 (C5-*C*H$_3$ or C5′-*C*H$_3$), 29.42 (C1-*C*H$_3$, C1′-*C*H$_3$), 34.01 (*C*4 or *C*4′), 34.12 (*C*4 or *C*4′), 35.27 (*C*1 or *C*1′), 35.30 (*C*1 or *C*1′), 40.78 (*C*2 or *C*2′), 40.80 (*C*2 or *C*2′), 58.18 (d, J = 7.2 Hz, N*C*H$_2$), 63.80 (*C*H$_2$OH), 64.29 (d, J = 4.5 Hz, NCH$_2$*C*H$_2$), 67.80 (d, J = 6.0 Hz, PO*C*H$_2$), 72.48 (d, J = 7.2 Hz, *C*HOHCH$_2$OH), 120.35 (*C*14), 121.35 (*C*14′), 127.13 (*C*12′), 127.23 (C13=*C*H), 129.75 (*C*7), 130.55 (*C*10′), 130.84 (*C*10 or *C*11), 130.89 (*C*10 or *C*11), 132.06 (*C*1 or *C*1′), 132.18 (*C*1 or *C*1′), 132.93 (*C*7′), 135.76 (*C*12), 138.44 (*C*8′), 138.94 (*C*6 or *C*6′), 138.95 (*C*6 or *C*6′), 139.07 (*C*8), 139.47 (*C*11′), 140.85 (*C*9), 146.37 (*C*15′), 146.85 (*C*9′), 149.11 (*C*13), 153.46 (*C*15), 154.88 (*C*13′); ESI-MS (%, rel. int.) *m/z* 768 (5.3, [M-H+Na]$^+$), 746 (100, [M]$^+$); HRESIMS: calcd for $C_{45}H_{65}NO_6P$ [M]$^+$, 746.4544; found, *m/z* 746.4542.

Hydrolysis of A2-GPE

A2-GPE (250 μG) was dissolved in DMSO (30 μL) and then added to 970 μL of DPBS buffer (with $CaCl_2$ and $MgCl_2$; GIBCO-Invitrogen, Carlsbad, CA) containing 300 units/mL phospholipase D (PLD, from *S. chromofuscus*; BIOMOL International, Plymouth Meeting, PA). The mixture was incubated for 2 hours at 37°C. A2-GPE and A2E were detected by UPLC as described above using gradient A.

A2-GPE Photo-Oxidation

A2E and A2-GPE (200 μL, 100 μM in DPBS with 1% DMSO) were irradiated (430 nm) for 0, 15, 30, 60, 120, and 240 seconds after which each sample was injected into the column (Waters XBridge C18) for analysis by UPLC-MS as described above with gradient A.

RESULTS

An *m/z* 746 Fluorophore in *Abca4*$^{-/-}$ Mouse and Human Eyes

The *Abca4* null mutant mouse serves as a model of autosomal recessive Stargardt disease and has been shown to accumulate the bisretinoid compounds of RPE lipofuscin in abundance.[7,16–18] We analyzed chloroform/methanol extracts of eyes of *Abca4*$^{-/-}$ mice by reversed-phase UPLC-MS with PDA detection at 430 nm. In addition to peaks in the UPLC profile having retention times readily assignable to the previously identified bisretinoids A2E and isoA2E[15–17] (Fig. 1A, B), a series of 4 peaks reflecting slightly less polar compounds was also observed. All peaks had absorbance spectra with two maxima; in the case of the most prominent peak, these maxima were 338 and 443 nm (Fig. 1A). All peaks also exhibited a molecular ion at *m/z* 746 (Fig. 1B) reflecting the same molecular weight. Online fluorescence monitoring showed that the peaks of interest were fluorescent compounds (Fig. 1A). Given their similar absorbance and identical molecular weight and based on our detection of multiple isomers of A2E,[15,19] we speculated that the major peak reflected a compound (subsequently known as A2-GPE) with double bonds in the *E*-configuration (all-*trans*). Accordingly, the less pronounced peaks were considered to be *Z*-isomers (*cis*-isomers) at various double bonds of the A2-GPE polyene side-chains. This postulate was confirmed by NMR (described below).

Due to shedding of photoreceptor outer segment membrane together with phagocytosis of RPE, the bisretinoids that form in photoreceptor cells do not accumulate there but instead are deposited in RPE. Thus for some Abca4$^{-/-}$ samples we removed neural retina from the remaining RPE/choroid/sclera. UPLC analysis indicated the presence of A2-GPE in the RPE/choroid/sclera samples, a finding reflecting accumulation in the RPE monolayer (Fig. 1C). Peaks with similar absorbance

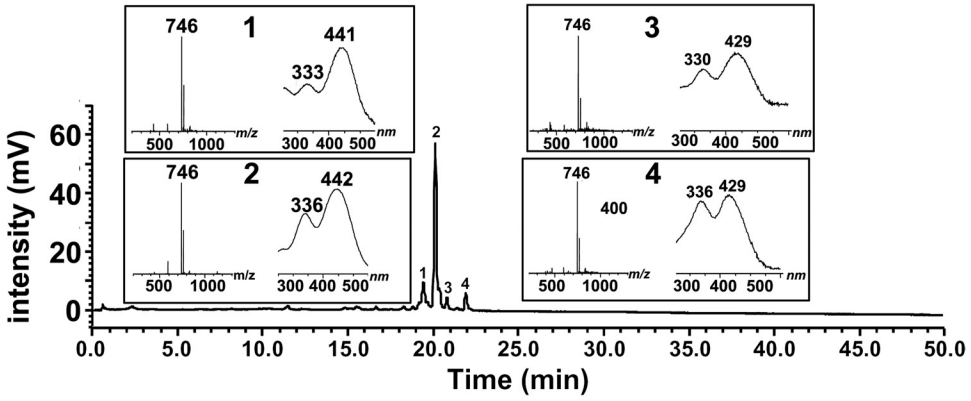

FIGURE 3. Reaction mixture of all-*trans*-retinal and glycerophosphoethanolamine. Incubation at room temperature for 3 days. Constituents of the synthetic mixture were separated by reversed-phase UPLC on a column (Waters XBridge C18; gradient B) with monitoring of UV-visible absorbance at 430 nm. *Insets*: selected ion monitoring at *m/z* 746 and UV-visible absorbance spectra corresponding to indicated chromatographic peak. Structure of A2-GPE, *right*.

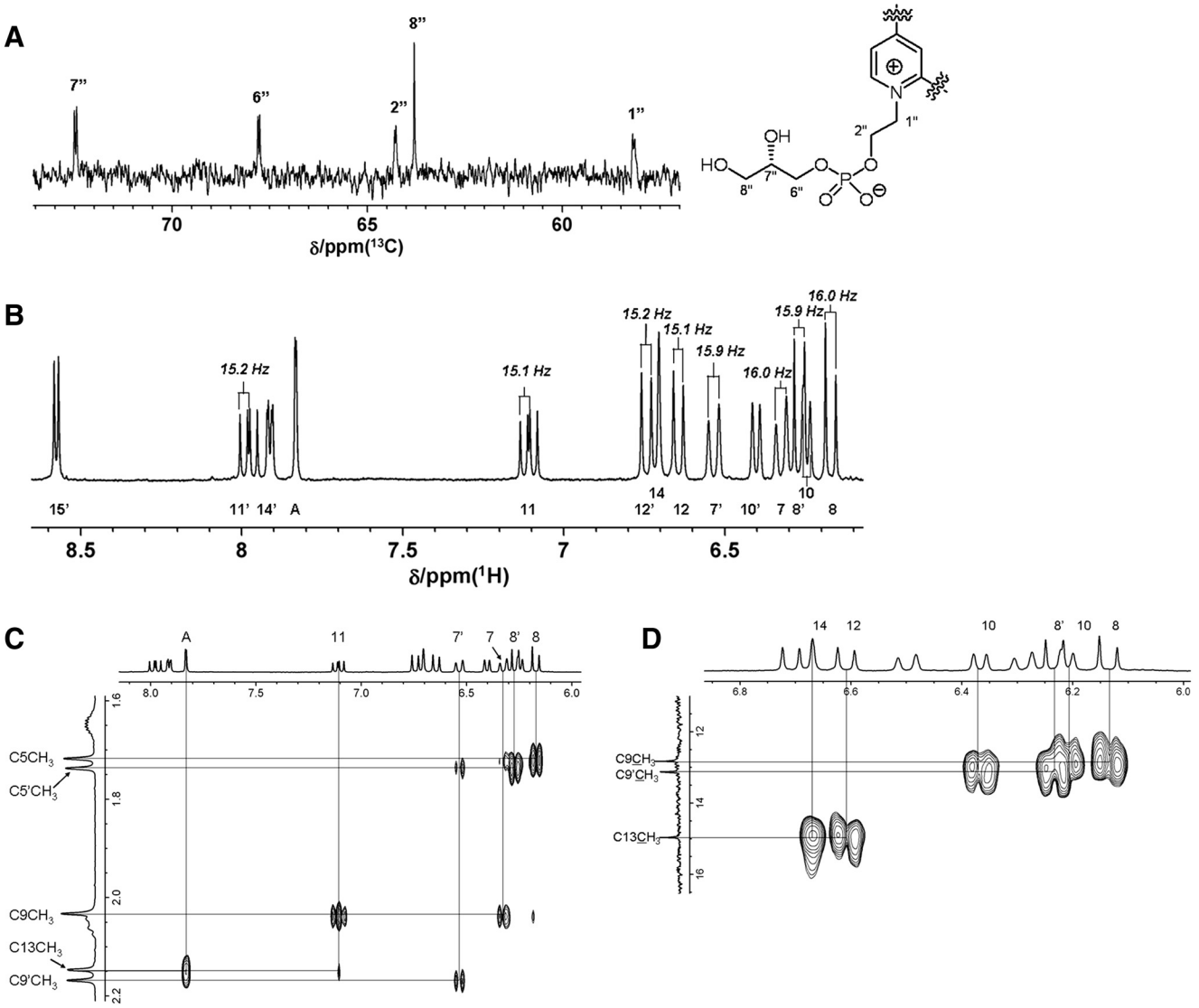

FIGURE 4. NMR spectra of A2-GPE. (**A**) Proton decoupled ^{13}C NMR spectra in CD_3OD. Signals appearing at 50 to 80 ppm are shown. Carbon resonances coupled with the phosphorous atom present as doublets. (**B**) ^{1}H NMR spectrum in CD_3OD. Signals within the 6.5–8.5 ppm region correspond to aromatic and olefinic protons. Critical coupling constants for the elucidation of the double bonds are presented. (**C**) Rotating-frame Overhauser effect spectroscopy (ROESY) spectra of A2-GPE in CD_3OD. A region showing the ROE correlations between olefinic protons and methyl protons is shown. ROE correlations appear when the two protons are sufficiently close geometrically. (**D**) A region of heteronuclear multiple-bond correlation spectroscopy (HMBC) spectrum of A2-GPE in CD_3OD. HMBC correlations were observed when the corresponding carbon and proton signals are within three, or occasionally four, bonds.

(338,446 nm) and the same molecular weight (*m/z* 746) were also detectable in samples of human RPE/choroid (Fig. 2A).

Analysis of Biosynthetic Reaction Mixtures

Given that the UV-visible spectra recorded by the PDA detector were similar to A2E and its precursor A2PE, we considered the possibility that the *m/z* 746 compounds were pyridinium bisretinoids forming by reaction with a lipid other than PE. The molecular weight of the compound led us to examine the product of reaction of all-*trans*-retinal and glycerophosphoethanolamine (A2-GPE). On incubating the reactants and analyzing by UPLC-MS, we observed a group of 4 compounds with retention times (19.0–21.9 minutes), PDA profiles (λ_{max}, 443 to 439 nm and 332 to 341 nm) and molecular ion signals (*m/z* 746) (Fig. 3) that were the same as the compounds in the mouse eyes (Fig. 1). The compound appearing at 19.88 minutes was the most prominent. The compound of interest in human RPE/choroid also exhibited a retention time corresponding to that of synthetic A2-GPE (Fig. 2B). The nomenclature, A2-GPE, was chosen to reflect a compound produced by reaction of two vitamin A (A2) and GPE.

Biomimetic synthesis of A2-GPE and subsequent preparative HPLC allowed us to obtain the major isomer in pure form and enabled NMR studies to reveal the full structure (Fig. 4). Signals corresponding to five protons were observed in the ^{1}H NMR spectrum of A2-GPE in CD_3OD, while these were absent in A2E. These protons were assigned to the glycerol moiety ($OC6''H_2C7''H(OH)C8''H_2OH$). The presence of this moiety was also disclosed by the ^{13}C-NMR spectrum. In addition to the 22 carbons corresponding to the A2E framework, three carbons resonances were detected as one singlet and two doublet signals in the proton decoupled ^{13}C NMR spectrum. Although proton decoupled ^{13}C NMR spectra are known to provide resonances as singlets, C1″, C2″, C6″, C7″ were observed as

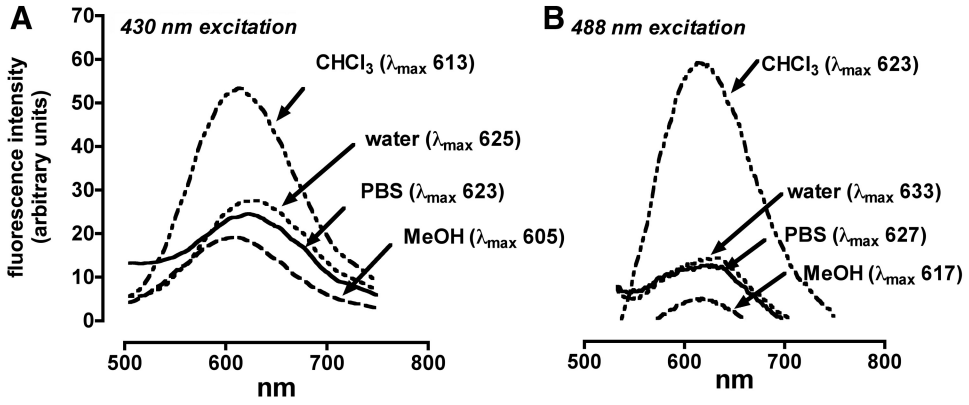

FIGURE 5. Fluorescent emission spectra of A2-GPE. (**A**) Excitation at 430 nm. (**B**) Excitation at 488 nm. Spectra were recorded in chloroform ($CHCl_3$), water (with 2% DMSO), DPBS (with 2% DMSO), and methanol (MeOH). Bandpass slit was 3 nm. Emission maxima (λ_{max}; nm) are indicated.

doublets in A2-GPE because of spin-spin couplings with the phosphorus atom (Fig. 4A). These findings were indicative of the presence of glycerophosphate in the molecule. The coupling constants for vicinal olefinic protons C7H/C8H, C11H/C12H, C7′H/C8′H, C11′H/C12′H were 16.0, 15.1, 15.9, 15.2 Hz, respectively, thus confirming the (*E*)-configuration for the double bonds (Fig. 4B). ROE correlations were found between AH/C13CH_3, C11H/C9CH_3 (Fig. 4C) thereby corroborating the (*E*)-stereochemistry for C9C10 and C13C14 double bonds. Although informative ROE correlations were not obtained for the C9′C10′ double bond, the C9′-methyl carbon resonance (13.19 ppm) was very close to that of the C9-methyl (12.89 ppm) in the ^{13}C NMR spectra. Because it has been established that chemical shifts in ^{13}C NMR spectra are sensitive to stereochemistry, these observations clearly indicated the (*E*)-configuration for the final C9′C10′ double bond. Assignment of these carbon signals was performed with the HMBC (hetero multiple bond correlation spectroscopy) (Fig. 4D). As described, these experiments established an (*E*)-stereochemical relationship for all double bonds in the side chain. Indeed, the signal profile for the olefinic protons in the ^1H NMR spectra resembled that of A2E but not isoA2E. The molecular ion was observed at *m/z* 746.4542 which confirms its molecular formula $C_{45}H_{65}NO_6P^+$ (theoretically 746.4544).

Quantitation of A2-GPE In Vivo

Quantitation of peak areas in UPLC chromatograms generated from eye cups harvested from albino *Abca4*$^{-/-}$ (Rpe65 Leu450) and wild type (Rpe65 Leu450) mice at 2, 4, and 6 months revealed an age-related increase in the pigment (Fig. 1D). By 6 months of age, A2-GPE levels in *Abca4*$^{-/-}$ mice were threefold higher than in wild type. Moreover, in wild type mouse eyes, A2E and A2-GPE were present in similar amounts (mean A2-GPE/mean A2E, 1.0) while in *Abca4* knockout mice, A2-GPE was twofold higher than A2E (mean A2-GPE/A2E, 2.2). In human RPE/choroid (45 and 54 years of age), A2E was considerably more abundant than A2-GPE (A2E: 854.8 and 1064.9 pmol per eye; A2-GPE 33.5 and 66.8 pmol per eye at 45 and 54 years of age, respectively).

Emission Spectra

Spectra recorded for A2-GPE varied according to the excitation wavelength used (430, or 488 nm) with excitation at the longer wavelength resulting in a red-shift in the emission maxima (Fig. 5). Fluorescence intensity, measured as area under the curve (AUC) at 430 nm excitation, also differed according to solvent used and was most intense in the nonpolar solvent chloroform (AUC, 7207), followed by water (AUC, 3991), DPBS (AUC, 3961), and methanol (AUC, 2671). The emission maxima were solvent-dependent and varied from 605 to 625 nm with excitation at 430 nm and from 617 to 633 nm with excitation at 488 nm.

Enzymatic Cleavage of A2-GPE

Phospholipase D catalyzes the hydrolysis of the phosphodiester bond of glycerophospholipids thereby generating phosphatidic acid and a free ethanolamine head-group. A2E is known to be generated by phospholipase-D-mediated phosphate hydrolysis of A2-PE.[19] A phospholipase-D activity has been reported as being present in photoreceptor outer segments.[20] We have also previously detected a phosphodiesterase activity in RPE lysosomes that can cleave A2PE.[21] Thus to demonstrate PLD-activity on A2-GPE, we incubated HPLC purified A2-GPE with the latter enzyme. As anticipated, the chromatographic peak that appeared was recognizable as A2E on the basis of absorbance maxima (λ_{max}, 440,337 nm) and mass (*m/z* 592) (Fig. 6).

Photo-Oxidation of A2-GPE

We compared the tendencies of A2-GPE and A2E to undergo photo-oxidation, by measuring the progressive loss of the two bisretinoids as irradiation time is lengthened. For these two bisretinoids, the pace of consumption was not appreciably different (Figs. 7A, 7B). To identify oxidized forms of the

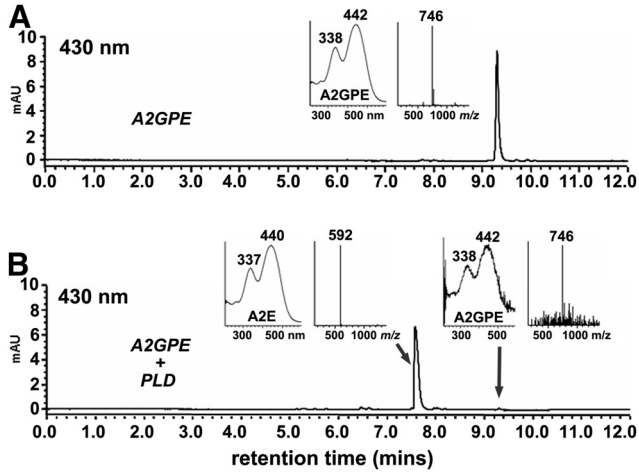

FIGURE 6. Hydrolysis of A2-GPE by PLD yields A2E. (**A**) A2-GPE without incubation. (**B**) A2-GPE sample after incubation with PLD. Starting compounds (A2-GPE) and cleavage products were detected by reversed phase UPLC-ESI-MS column (Waters XBridge) and monitoring at 430 nm (gradient A). *Insets*: UV-visible absorbance and selected ion monitoring of the indicated compounds. PLD cleaves at the phosphodiester bond in A2-GPE to release A2E.

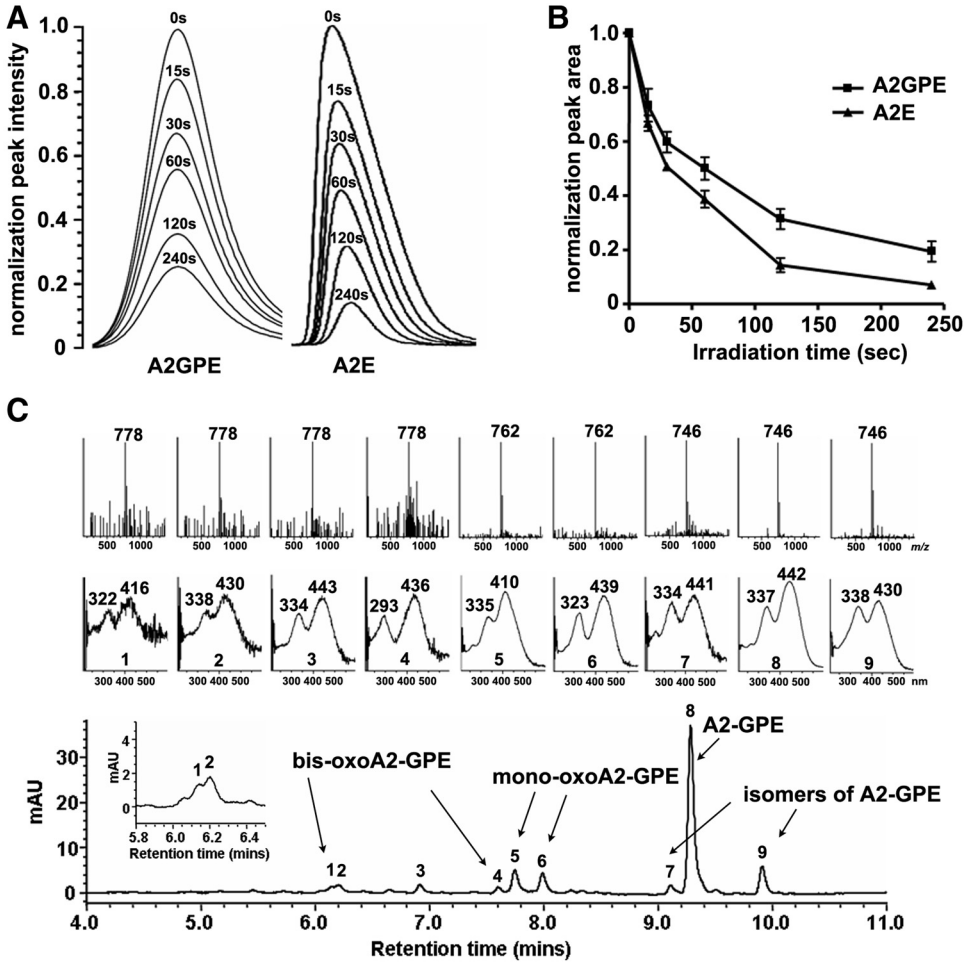

FIGURE 7. Photo-oxidation of A2-GPE and A2E. (**A**) Photo-oxidation-associated consumption of A2-GPE presented as declining chromatographic peak intensity (absorbance monitoring) with different irradiation (430 nm) times (seconds, s). (**B**) Plots of normalized peak areas. (**C**) Representative reversed-phase UPLC chromatogram with selected ion monitoring of mass (*Inset*, *above*) and absorbance (*Inset*, *below*) (gradient A). A2-GPE, *m/z* 746; monooxoA2-GPE, *m/z* 762; bisoxoA2-GPE, *m/z* 778.

bisretinoid, we irradiated samples of A2-GPE (*m/z* 746) and analyzed by UPLC with MS monitoring to detect changes in molecular weight reflecting the addition of oxygens (*m/z* 762 or 778; addition of one and two oxygens, respectively) and with UV-visible spectroscopy to detect hypsochromic absorbance shifts reflecting oxidation-associated loss of double bond conjugation. Six peaks were observed to elute earlier than A2-GPE as is expected due to oxidation-associated increased polarity. Two of these peaks (Fig. 7C) likely reflect the addition of two oxygens to form endoperoxides on the long (peak 1) and short (peak 4) arms of the molecule, because in both cases the *m/z* value was 778 (746 + (2 × 16) and the hypsochromic absorbance shift (approximately 30 nm) was indicative of the loss of one double bond. Another peak exhibiting *m/z* 762 (746 + 16), probably represented an oxidized species formed by the addition of a single oxygen on the long arm (peak 5). In addition, there were three peaks (e.g., peaks 2, 3, and 6) associated with a mass consistent with the addition of oxygens, yet an absorbance shift of the expected size was not apparent. The structure of this species has not yet been determined. However, we note that endoperoxide opening with proton donation to form a diol followed by radical reaction and elimination of water could re-establish the conjugated double bonds.[22]

DISCUSSION

We have shown that in addition to bisretinoid formation on PE, the bisretinoid mixture in RPE cells includes GPE derivatized by a pair of vitamin A aldehydes; thus the nomenclature A2-GPE. The structure of the bisretinoid A2-GPE has been demonstrated by mass spectrometry and NMR spectroscopy together with biomimetic synthesis. The ^{1}H-NMR and ^{13}C-NMR spectra of A2-GPE confirmed the presence of the glycerol and phosphate moieties. Other structural features, in particular, the pyridinium ring, are clearly shared with A2E because PLD-mediated phosphate cleavage of A2-GPE yields A2E. The fluorescent bisretinoid, A2-GPE accumulates with age in RPE cells.

GPE is the ethanolamine ester of glycerophosphoric acid. In human retina, levels of glycerophosphoethanolamine are 22% of phosphatidylethanolamine,[23] a content that is appreciable, although the significance of this relatively high content is not understood. GPE is the major product of PE catabolism and is released as a result of phospholipase A-mediated cleavage of the acyl chains at both the *sn-1* and *sn-2* position of the glycerol backbone; further hydrolysis can yield ethanolamine and glycerophosphate. GPE can also be generated from plasmalogens,[24] a class of glycerophospholipid with a vinyl-ether moiety at the *sn*-1-position of the glycerol backbone; plasmalogens are highly susceptible to oxidation. Thus A2-GPE may form by direct bisretinoid adduction on GPE or it may be generated secondary to A2PE catabolism. Direct bisretinoid adduct formation on GPE would indicate that in addition to A2-adducts on PE, glycerophosphoethanolamine is available for reaction. In the presence of *Abca4* deficiency the increase in A2-GPE is pronounced, even relative to A2E. This increase in A2-GPE could occur due to increased formation of A2PE (a known outcome of *Abca4* deficiency) followed by increased

phospholipase A-mediated cleavage of A2PE. Alternatively, increased A2-GPE in the *Abca4* null mutant may reflect direct reaction of all-*trans*-retinal with A2-GPE. The latter is the most parsimonious explanation because *Abca4* is not known to intersect the phospholipase A pathway.

We have demonstrated in an in vitro assay, that phospholipase D activity can cleave A2-GPE to generate A2E. This finding indicates that A2-GPE, like the phosphatidylethanolamine-bisretinoid A2PE, can serve as a precursor of A2E.[21] However, because A2-GPE accumulates with age, phospholipase D-mediated cleavage of A2-GPE is not necessarily the rule. In our experience, A2-GPE elutes from an HPLC column (C18 Sep-Pak, Millipore) as a broad peak appearing later than our typical running times. It is perhaps for this reason that we did not detect A2-GPE in previous chromatographic analyses by HPLC. Conversely, different column features together with a higher pressure enabled a sharp peak by UPLC.

The accumulation of bisretinoid by RPE is well known to have adverse consequences for the cell and is implicated in disease processes leading to macular degeneration, both the recessive Stargardt disease and the age-related form (AMD).[25] The identification of individual bisretinoid components is important because this information increases awareness of the burden placed on the RPE cell by the accumulation of these retinoid-derived compounds. Investigations of potential treatments for macular degeneration include approaches that would reduce bisretinoid formation.[26] Improved understanding of the biosynthetic pathways and the properties of the bisretinoids could broaden the therapeutic possibilities.

References

1. Fliesler SJ, Anderson RE. Chemistry and metabolism of lipids inthe vertebrate retina. *Prog Lipid Res.* 1983;22:79–131.
2. Anderson RE, Maude MB. Phospholipids of bovine outer segments. *Biochemistry.* 1970;9:3624–3628.
3. Boesze-Battaglia K, Schimmel RJ. Cell membrane lipid composition and distribution: implications for cell function and lessons learned from photoreceptors and platelets. *J Exp Biol.* 1997;200:2927–2936.
4. Gibson NJ, Brown MF. Membrane lipid influences on the energetics of the metarhodopsin I and metarhodopsin II conformational states of rhodopsin probed by flash photolysis. *Photochem Photobiol.* 1991;54:985–992.
5. Alves ID, Salgado GF, Salamon Z, Brown MF, Tollin G, Hruby VJ. Phosphatidylethanolamine enhances rhodopsin photoactivation and transducin binding in a solid supported lipid bilayer as determined using plasmon-waveguide resonance spectroscopy. *Biophys J.* 2005;88:198–210.
6. Jastrzebska B, Goc A, Golczak M, Palczewski K. Phospholipids are needed for the proper formation, stability, and function of the photoactivated rhodopsin-transducin complex. *Biochemistry.* 2009;48:5159–5170.
7. Weng J, Mata NL, Azarian SM, Tzekov RT, Birch DG, Travis GH. Insights into the function of Rim protein in photoreceptors and etiology of Stargardt's disease from the phenotype in abcr knockout mice. *Cell.* 1999;98:13–23.
8. Allikmets R, Shroyer NF, Singh N, et al. Mutation of the Stargardt disease gene (ABCR) in age-related macular degeneration. *Science.* 1997;277:1805–1807.
9. Wu L, Nagasaki T, Sparrow JR. Photoreceptor cell degeneration in Abcr$^{-/-}$ mice. *Adv Exp Med Biol.* 2010;664:533–539.
10. Maeda A, Maeda T, Imanishi Y, et al. Role of photoreceptor-specific retinol dehydrogenase in the retinoid cycle in vivo. *J Biol Chem.* 2005;280:18822–18832.
11. Maeda A, Maeda T, Imanishi Y, et al. Retinol dehydrogenase (RDH12) protects photoreceptors from light-induced degeneration in mice. *J Biol Chem.* 2006;281:37697–37704.
12. Chrispell JD, Feathers KL, Kane MA, et al. Rdh12 activity and effects on retinoid processing in the murine retina. *J Biol Chem.* 2009;284:21468–21477.
13. Vasireddy V, Jablonski MM, Khan NW, et al. Elovl4 5-bp deletion knock-in mouse model for Stargardt-like macular degeneration demonstrates accumulation of ELOVL4 and lipofusin. *Exp Eye Research.* 2009;89:905–912.
14. Wu Y, Fishkin NE, Pande A, Pande J, Sparrow JR. Novel lipofuscin bisretinoids prominent in human retina and in a model of recessive Stargardt disease. *J Biol Chem.* 2009;284:20155–20166.
15. Parish CA, Hashimoto M, Nakanishi K, Dillon J, Sparrow JR. Isolation and one-step preparation of A2E and iso-A2E, fluorophores from human retinal pigment epithelium. *Proc Natl Acad Sci U S A.* 1998;95:14609–14613.
16. Mata NL, Weng J, Travis GH. Biosynthesis of a major lipofuscin fluorophore in mice and humans with ABCR-mediated retinal and macular degeneration. *Proc Natl Acad Sci U S A.* 2000;97:7154–7159.
17. Kim SR, Fishkin N, Kong J, Nakanishi K, Allikmets R, Sparrow JR. The Rpe65 Leu450Met variant is associated with reduced levels of the RPE lipofuscin fluorophores A2E and iso-A2E. *Proc Natl Acad Sci U S A.* 2004;101:11668–11672.
18. Kim SR, Jang YP, Jockusch S, Fishkin NE, Turro NJ, Sparrow JR. The all-trans-retinal dimer series of lipofuscin pigments in retinal pigment epithelial cells in a recessive Stargardt disease model. *Proc Natl Acad Sci U S A.* 2007;104:19273–19278.
19. Ben-Shabat S, Parish CA, Vollmer HR, et al. Biosynthetic studies of A2E, a major fluorophore of RPE lipofuscin. *J Biol Chem.* 2002;277:7183–7190.
20. Salvador GA, Giusto NM. Characterization of phospholipase D activity in bovine photoreceptor membranes. *Lipids.* 1998;33:853–860.
21. Sparrow JR, Kim SR, Cuervo AM, Bandhyopadhyayand U. A2E, a pigment of RPE lipofuscin is generated from the precursor A2PE by a lysosomal enzyme activity. *Adv Exp Med and Biol.* 2008;613:393–398.
22. Steenken S, Davies MJ, Gilbert BC. Pulse radiolysis and election spin resonance studies of the dehydration of radicals fro 1,2-diols and related compounds. *J Chem Soc Perkin Trans.* 1986;2:1003–1010.
23. Alberghina M, Giacchetto A, Cavallaro N. Levels of ethanolamine intermediates in the human and rat visual system structures: Comparison with neural tissues of a lower vertebrate (Mustelus canis) and an invertebrate (Loligo pealei). *Neurochem Int.* 1993;22:45–51.
24. Lessig J, Fuch B. HOCl-mediated glycerophosphocholine and glycerophosphoethanolamine generation from plasmalogens in phospholipid mixtures. *Lipids.* 2010;45:37–51.
25. Sparrow JR, Wu Y, Kim CY, Zhou J. Phospholipid meets all-trans-retinal: the making of RPE bisretinoids. *J Lipid Res.* 2010;51:247–261.
26. Zarbin MA, Rosenfeld PJ. Pathway-based therapies for age-related macular degeneration. An integrated survey of emerging treatment alternatives. *Retina.* 2010;30:1350–1367.